



PRDM16 represses the type I interferon response in adipocytes to promote mitochondrial and thermogenic programming

Megan Kissig^{1,2}, Jeff Ishibashi^{1,2}, Matthew J Harms^{1,2}, Hee-Woong Lim^{1,3} , Rachel R Stine^{1,2},
Kyoung-Jae Won^{1,3} & Patrick Seale^{1,2,*} 

Abstract

Brown adipose has the potential to counteract obesity, and thus, identifying signaling pathways that regulate the activity of this tissue is of great clinical interest. PRDM16 is a transcription factor that activates brown fat-specific genes while repressing white fat and muscle-specific genes in adipocytes. Whether PRDM16 also controls other gene programs to regulate adipocyte function was unclear. Here, we identify a novel role for PRDM16 in suppressing type I interferon (IFN)-stimulated genes (ISGs), including *Stat1*, in adipocytes *in vitro* and *in vivo*. Ectopic activation of type I IFN signaling in brown adipocytes induces mitochondrial dysfunction and reduces uncoupling protein 1 (UCP1) expression. *Prdm16*-deficient adipose displays an exaggerated response to type I IFN, including higher STAT1 levels and reduced mitochondrial gene expression. Mechanistically, PRDM16 represses ISGs through binding to promoter regions of these genes and blocking the activating function of IFN regulatory factor 1 (IRF1). Together, these data indicate that PRDM16 diminishes responsiveness to type I IFN in adipose cells to promote thermogenic and mitochondrial function.

Keywords brown adipose; interferon regulatory factor; mitochondria; *Prdm16*; *Ucp1*

Subject Categories Immunology; Metabolism

DOI 10.15252/embj.201695588 | Received 26 August 2016 | Revised 15 March 2017 | Accepted 19 March 2017 | Published online 13 April 2017

The EMBO Journal (2017) 36: 1528–1542

Introduction

There are three general classes of adipocytes: white, brown, and beige. White adipocytes store and release energy according to systemic demand, whereas brown and beige adipocytes burn energy to produce heat. Brown and beige adipocytes are characterized by a high density of mitochondria that contain uncoupling protein 1 (UCP1) in their inner membrane. UCP1, when activated by fatty

acids, permits proton leak across the inner mitochondrial membrane (Klingenberg *et al*, 1999). Dissipation of the mitochondrial proton gradient by UCP1 drives the oxidation of available substrates and results in heat production. The thermogenic function of brown and beige fat defends mammals against hypothermia upon cold exposure. Additionally, brown and beige fat activity counteracts many of the harmful metabolic effects of a high-fat diet in mice, including obesity and insulin resistance (Guerra *et al*, 1998; Cederberg *et al*, 2001; Feldmann *et al*, 2009; Seale *et al*, 2011; Auffret *et al*, 2012). In humans, brown adipose tissue (BAT) activity levels correlate with leanness (van Marken Lichtenbelt *et al*, 2009; Saito *et al*, 2009).

PRD1-BF1-RIZ1 homologous domain-containing protein 16 (PRDM16) is a critical regulator of the brown fat-selective gene program in brown and beige adipocytes (Seale *et al*, 2007, 2008, 2011; Kajimura *et al*, 2008; Ohno *et al*, 2012; Harms *et al*, 2015). PRDM16 increases the transcription of brown fat-specific genes such as *Ucp1* by co-activating various transcription factors, including peroxisome proliferator-activated receptor gamma (PPAR γ), PPAR γ coactivator 1-alpha (PGC1 α), and CCAAT/enhancer-binding protein beta (CEBP- β) (Seale *et al*, 2007, 2008; Kajimura *et al*, 2009). The co-activator function of PRDM16 is mediated, at least in part, through recruitment of the Mediator complex to brown fat-specific gene enhancers (Harms *et al*, 2015; Iida *et al*, 2015). PRDM16 also represses the transcription of certain white adipocyte-specific and muscle-specific genes in adipose cells by interacting with C-terminal-binding proteins (CtBPs) and euchromatic histone-lysine N-methyltransferase 1 (EHMT1) (Kajimura *et al*, 2008; Ohno *et al*, 2013; Harms *et al*, 2014). Of note, the N-terminal PR domain of PRDM16 contains methyltransferase activity and is able to methylate histone H3K9 (Pinheiro *et al*, 2012; Li *et al*, 2015; Zhou *et al*, 2016).

Genetic loss-of-function studies in mice show that PRDM16 is required for the maintenance of BAT activity and for beige adipocyte biogenesis in white adipose tissue (WAT) (Seale *et al*, 2011; Cohen *et al*, 2014; Harms *et al*, 2014). PRDM16 also plays an important role in the development and function of other cell types, including

¹ Institute for Diabetes, Obesity & Metabolism, Smilow Center for Translational Research, Perelman School of Medicine, University of Pennsylvania, Philadelphia, PA, USA

² Department of Cell and Developmental Biology, Smilow Center for Translational Research, Perelman School of Medicine, University of Pennsylvania, Philadelphia, PA, USA

³ Genetics Department, Smilow Center for Translational Research, Perelman School of Medicine, University of Pennsylvania, Philadelphia, PA, USA

*Corresponding author. Tel: +1 215 573 8856; Fax: +1 215 898 5408; E-mail: sealep@upenn.edu

hematopoietic stem cells (HSCs) and neural stem cells (NSCs) (Chuikov *et al*, 2010; Aguilo *et al*, 2011). Deletion of PRDM16 in HSCs and NSCs increases the levels of reactive oxygen species (ROS) and promotes cell death (Chuikov *et al*, 2010). Similarly, loss of PRDM16 in astrocytoma cells leads to mitochondrial dysfunction and apoptosis (Lei *et al*, 2016). In HSCs, PRDM16 induces the expression of Mitofusin 2 to promote mitochondrial function and reduce endoplasmic reticulum stress (Luchsinger *et al*, 2016).

In this study, we identify a previously unrecognized role for PRDM16 as a repressor of type I interferon (IFN) responses. The type I IFN pathway is best known for its critical role in antiviral defense. However, type I IFN also regulates the activity of certain stem cell populations (Essers *et al*, 2009; Sato *et al*, 2009; Yu *et al*, 2015). We found that PRDM16 blocked both the basal and IFN α -induced expression of type I IFN-stimulated genes (ISGs) in adipogenic cells. Conversely, deletion of *Prdm16* from brown adipose cells and from BAT *in vivo* increased ISG expression. *Prdm16*-deficient BAT was also hyper-responsive to induced IFN signaling *in vivo*. Ectopic activation of type I IFN signaling in brown adipocytes caused profound mitochondrial dysfunction and reduced thermogenic capacity. Mechanistically, PRDM16 blocked the binding and transcriptional activating function of IFN regulatory factor 1 (IRF1) at ISG promoters. We conclude that PRDM16-mediated ISG repression plays an important role in maintaining mitochondrial and thermogenic function in adipocytes.

Results

PRDM16 is required to repress type I IFN-stimulated genes (ISGs) in adipocytes

PRDM16 binds and activates the transcription of many brown fat-specific genes in adipocytes (Harms *et al*, 2015). To identify additional PRDM16-regulated genes in adipocytes, we performed an unbiased analysis of gene expression in *Prdm16*-deleted versus control adipocytes using cDNA microarrays. Adipogenic precursor cells were isolated from the inguinal (subcutaneous) WAT (ingWAT) of *Rosa26^{CreER}; Prdm16^{fllox} (R26^{Cre+})* mice and treated with 4-hydroxytamoxifen (4OHT) to induce *Prdm16* deletion or with vehicle (ethanol) as control. *Prdm16*-knockout (KO) and control cells were then induced to undergo adipocyte differentiation in the presence or absence of the PPAR γ ligand rosiglitazone (rosi), which activates mitochondrial and brown fat-selective genes (Tai *et al*, 1996; Digby *et al*, 1998; Petrovic *et al*, 2008; Ohno *et al*, 2012). *Prdm16* KO and control cells underwent efficient conversion into mature lipid droplet-containing adipocytes that expressed equivalent levels of general adipocyte-specific genes such as *Adiponectin* (*AdipoQ*) and *Pparg2* (Fig 1A). *Prdm16*-deleted adipocytes expressed drastically reduced levels of *Ucp1* and other brown fat-selective genes in response to rosi (Fig 1A), in agreement with published results (Ohno *et al*, 2012).

Global analyses revealed that many brown fat-selective and mitochondrial genes were induced by rosi in a PRDM16-dependent manner (Figs 1B and EV1A; green cluster). Gene ontology (GO) analysis of the most upregulated genes in *Prdm16* KO versus control adipocytes, both with and without rosi treatment, identified the type

I IFN and viral defense pathways as prominent PRDM16-repressed pathways (Fig 1B and C; blue cluster). The majority of the genes in this group were ISGs, including *Irf7*, *Ifi44*, *Mx2*, *Cxcl9*, and *Oas2*. These ISGs were also greatly increased in 4OHT-treated adipocytes from *R26^{Cre+}* but not from *Prdm16^{fl/fl}* wild-type mice, showing that ISG activation was not caused by 4OHT (Fig EV1B). Importantly, ISG levels were increased in *Prdm16* KO BAT of adult *Myf5^{Cre}; Prdm16^{fl/fl}* mice compared to control WT BAT (Fig 1D). The induction of ISGs was not apparent in the BAT of young *Prdm16* KO mice (Fig EV1C), which have intact thermogenic function (Harms *et al*, 2014). Additionally, the cold-induced beiging of subcutaneous inguinal (ing) WAT, which occurs in a PRDM16-dependent manner (Cohen *et al*, 2014), was accompanied by decreased expression levels of many ISGs, including *Ifi272l2* and *Ccl5* (Fig EV1D).

PRDM16 expression increases during the course of adipocyte differentiation (Seale *et al*, 2007, 2011), and thus, the role of PRDM16 in regulating genes at the preadipocyte stage is largely unknown. We reliably detected nuclear PRDM16 protein in precursor cells isolated from the ingWAT of WT mice, while the addition of 4OHT eliminated PRDM16 protein signal only from *R26^{Cre+}*-derived cells (Fig 1E). As observed in mature adipocytes, *Prdm16* deletion in ingWAT-derived (Fig 1F) and BAT-derived (Fig EV1E) precursor cells led to increased expression of many ISGs. Similarly, CRISPR/Cas9-mediated reduction in PRDM16 (PRDM16-CRISPR) expression in brown adipocyte precursors increased ISG expression (Fig EV1F). Together, these results establish a requirement for PRDM16 in repressing a broad set of type I ISGs in adipocytes and adipocyte precursor cells both *in vitro* and *in vivo*.

PRDM16 blocks type I IFN responses downstream of IFNAR receptor

To determine whether ectopic PRDM16 expression is sufficient to repress ISGs, we transduced *Prdm16* KO brown adipocyte precursors with either control or PRDM16-expressing retroviral vectors. PRDM16 decreased both the mRNA and protein levels of signal transducer and activator of transcription 1 and 2 (STAT1 and STAT2) (Fig 2A and B), which are transcription factors that mediate many effects of type I IFN (Leung *et al*, 1995; Bromberg *et al*, 1996; Horvath *et al*, 1996; Meraz *et al*, 1996; Park *et al*, 2000). The reduced protein levels of STAT1 and STAT2 corresponded with reduced levels of the phosphorylated (active) forms of these factors (Fig 2B). PRDM16 also strongly blocked the expression of many other ISGs, including a 10- to 20-fold reduction in the mRNA levels of *Irf7*, *Ifi44*, *Oas2*, and *Oas3* (Fig 2A). PRDM16 did not reduce the levels of STAT3, another transcription factor involved in the IFN cascade (Fig 2B).

We next examined whether PRDM16 regulates transcriptional responses to exogenous type I IFN. Ectopic PRDM16 expression reduced basal ISG levels and blunted IFN α -induced ISG expression, including *Stat1* and *Stat2* (Fig 2C). Conversely, ISGs were induced to higher levels in *Prdm16* KO cells than in control cells upon treatment with varying doses of IFN α (Fig EV2A), indicating that *Prdm16* deficiency sensitizes cells to IFN α .

Type I IFNs bind to the interferon alpha and beta receptor (IFNAR) on the cell surface which activates a downstream signaling cascade. This response can be efficiently and specifically blocked in

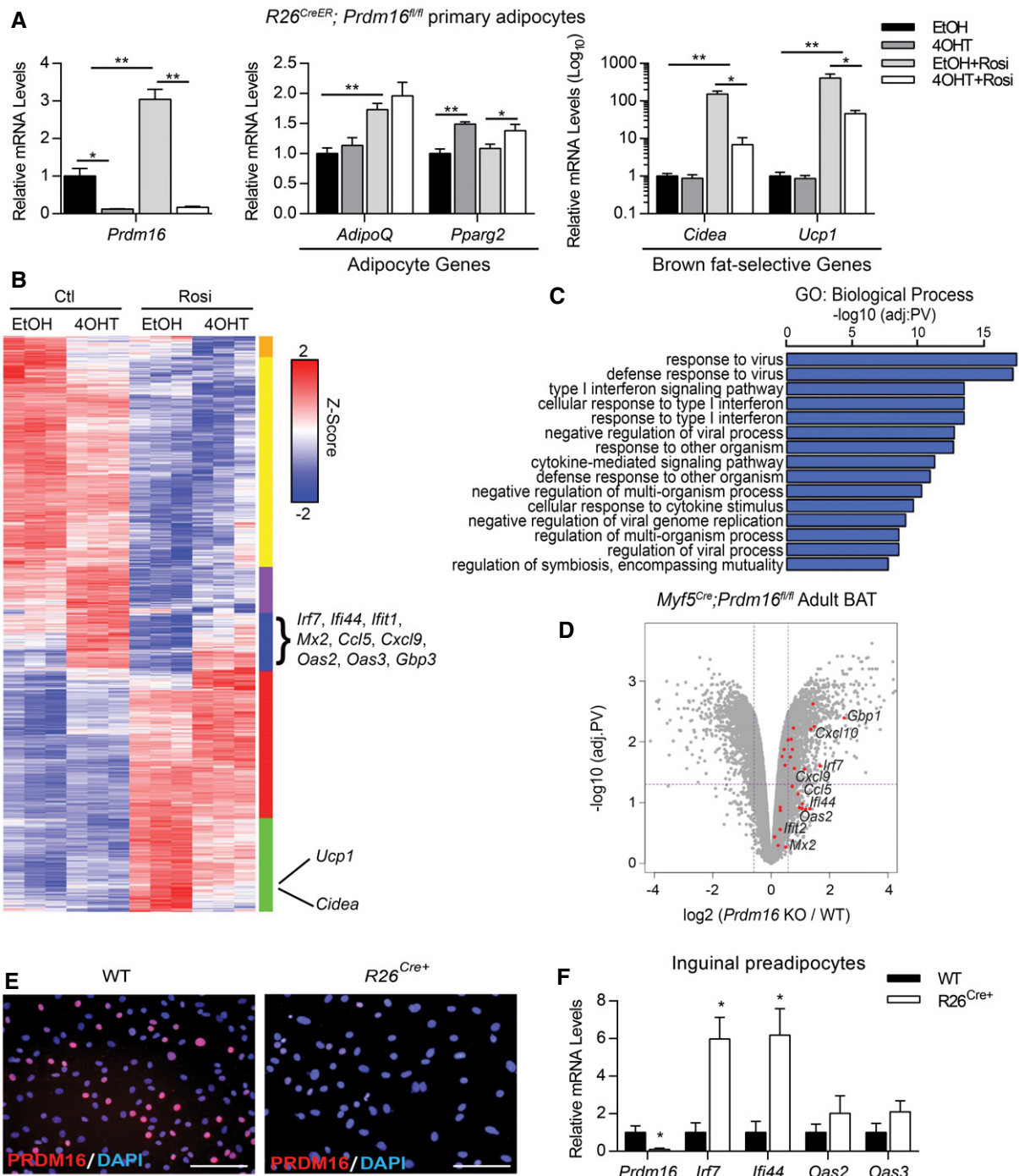


Figure 1. PRDM16 is required to repress type I IFN-stimulated genes (ISGs) in adipocytes.

A Relative mRNA levels of *Prdm16*, pan-adipogenic genes (*AdipoQ*, *Pparg2*), and brown fat-selective genes (*Cidea*, *Ucp1*) in *R26^{CreER}; Prdm16^{fl/fl}* inguinal adipocytes treated with ethanol (EtOH) or 1 μM 4-hydroxytamoxifen (4OHT) to induce knockdown of *Prdm16*, then differentiated +/- 1 μM rosiglitazone (rosi).

B Heat map depicting global gene expression levels in control (EtOH) and *Prdm16* KO (4OHT) cells under control (Ctl) or rosi treatment.

C Gene ontology (GO) analysis of upregulated genes (blue cluster, B).

D Volcano plot depicting log-fold change of gene expression in *Prdm16^{fl/fl}* (WT) and *Myf5^{Cre}; Prdm16^{fl/fl}* (KO) adult mice. Red dots identify type I IFN-stimulated genes (ISGs) found in the blue cluster of the heat map in (B).

E Immunofluorescence analysis of PRDM16 expression (red) and nuclei (DAPI, blue) in WT and *R26^{CreER}; Prdm16^{fl/fl}* (*R26^{Cre+}*) primary inguinal preadipocytes treated with 4OHT. Scale bar = 100 μm .

F Relative mRNA levels of *Prdm16* and ISGs in WT and *R26^{Cre+}* primary inguinal preadipocytes.

Data information: In (A, F), data represent ($n = 3$) mean \pm standard deviation and are consistent with results from triplicate independent experiments. * $P < 0.05$, ** $P < 0.01$ (Student's *t*-test).

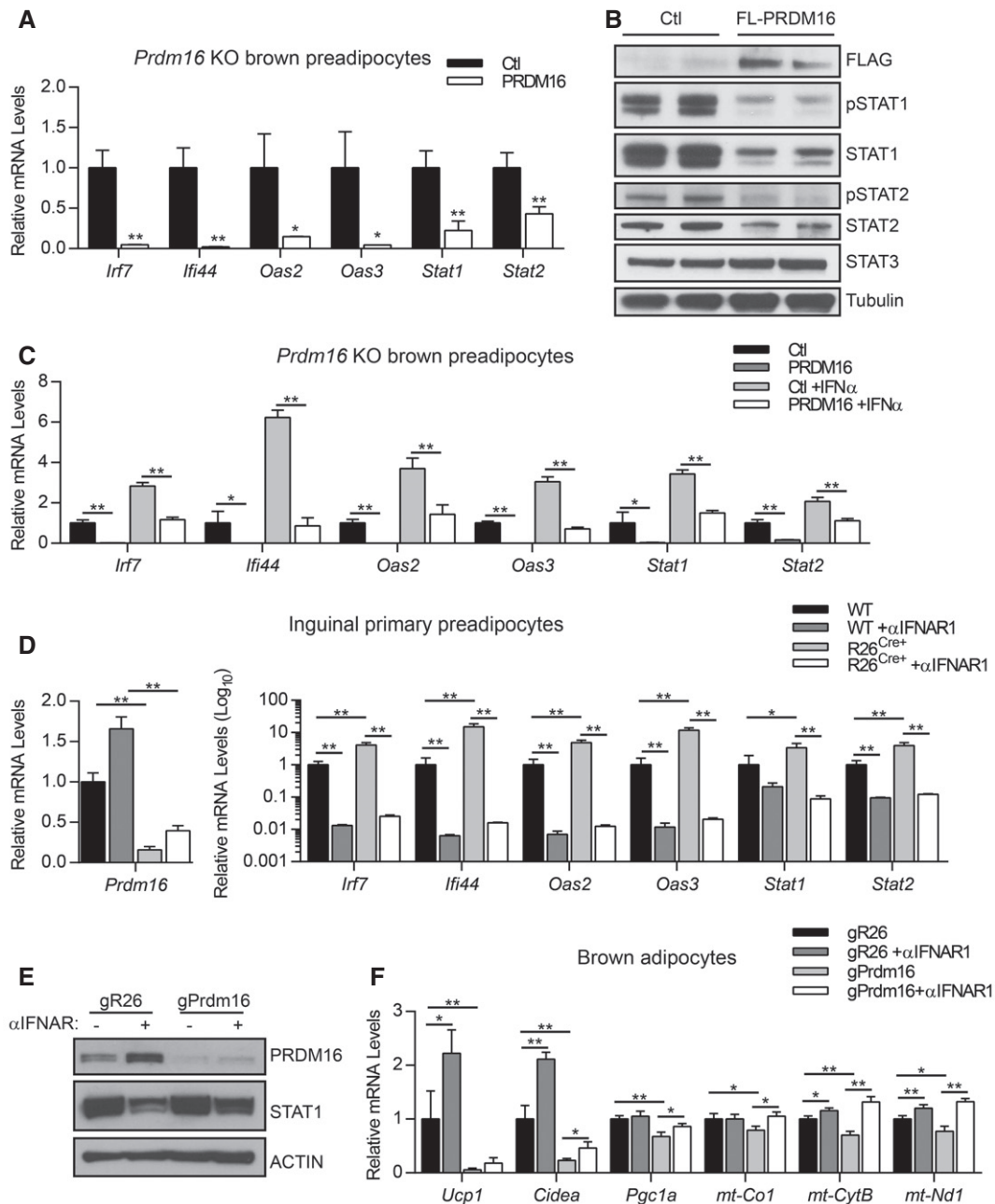


Figure 2. PRDM16 blocks type I IFN signaling downstream of IFNAR receptor.

- A Relative mRNA levels of IFN-stimulated genes (ISGs) in *Prdm16* KO brown adipocyte precursors infected with control (Ctl) or PRDM16 retrovirus. Data represent ($n = 3$) mean \pm standard deviation and are consistent with results from duplicate independent experiments. * $P \leq 0.05$, ** $P \leq 0.01$ (Student's *t*-test).
- B Western blot analysis of FLAG, phosphorylated STAT1 (pSTAT1), STAT1, phosphorylated STAT2 (pSTAT2), STAT3, and tubulin (loading control) protein in *Prdm16* KO precursors infected with control (Ctl) or FLAG-PRDM16 retrovirus.
- C Relative mRNA levels of ISGs in control (Ctl) and PRDM16-expressing preadipocytes +/- recombinant mouse IFN α . Data represent ($n = 3$) mean \pm standard deviation and are consistent with results from duplicate independent experiments. * $P \leq 0.05$, ** $P \leq 0.01$ (Student's *t*-test).
- D Relative mRNA levels of ISGs in WT and R26^{Cre+} inguinal preadipocytes treated with 4OHT and vehicle or anti-IFNAR1 neutralizing antibody (α IFNAR1) for 4 days. Data represent ($n = 3$) mean \pm standard deviation and are consistent with results from duplicate independent experiments. * $P \leq 0.05$, ** $P \leq 0.01$ (paired two-way ANOVA).
- E Western blot analysis of PRDM16, STAT1, and actin (loading control) protein in brown adipocytes expressing gR26 (control) and gPrdm16 CRISPR/Cas9 constructs and treated +/- α IFNAR1 throughout differentiation.
- F Relative mRNA levels of brown-selective (*Ucp1*, *Cidea*, *Pgc1a*) and mitochondrial (*mt-Co1*, *mt-CytB*, *mt-Nd1*) genes in brown adipocytes expressing gR26 and gPrdm16 CRISPR/Cas9 constructs +/- α IFNAR1 throughout differentiation. Data represent ($n = 3$) mean \pm standard deviation and are consistent with results from duplicate independent experiments. * $P \leq 0.05$, ** $P \leq 0.01$ (paired two-way ANOVA).

Source data are available online for this figure.

brown preadipocytes through treatment with an IFNAR-neutralizing antibody (α IFNAR) (Fig EV2B). Notably, α IFNAR1 treatment eliminated ISG expression in both WT and *Prdm16* KO cells, indicating that receptor signaling is active under basal conditions and that ISG induction due to loss of PRDM16 requires IFNAR function (Fig 2D).

To determine whether basal IFN signaling influences brown adipogenesis, we differentiated control and PRDM16-depleted brown preadipose cells with or without α IFNAR1. PRDM16 expression was efficiently reduced using CRISPR/Cas9 technology (Fig 2E), resulting in a corresponding decrease in the levels of brown fat-specific (*Ucp1*, *Cidea*, *Pgc1a*) and mitochondrial (*mt-Co1*, *mt-CytB*, *mt-Nd1*) genes in differentiated brown adipocytes (Fig 2F). Anti-IFNAR treatment rescued the expression of mitochondrial genes but not *Ucp1* in *Prdm16*-deleted adipocytes (Fig 2F). Altogether, these results demonstrate that PRDM16 acts downstream of the type I IFN receptor to repress transcriptional responses to type I IFN and safeguard mitochondrial gene expression in adipocytes.

Activation of type I IFN signaling disrupts mitochondrial structure and function in adipocytes

The above studies suggested that IFN activation may have an inhibitory effect on brown fat cell differentiation and/or function. To evaluate this, we treated brown adipocyte precursor cells with recombinant IFN α or vehicle control and induced adipocyte differentiation. We used a dose of IFN α that increased STAT1 mRNA and protein levels and elevated ISG levels to a similar extent as that observed in *Prdm16* KO cells (Fig 3A and C). A previous study reported that IFN α inhibits adipogenesis of 3T3-L1 cells (Lee *et al*, 2016). By contrast, we found that IFN α -treated and control-treated cells differentiated into Oil-Red-O-stained mature adipocytes with equivalent efficiency and expressed similar levels of the general adipocyte marker genes *Fabp4* and *Pparg2* (Fig 3B). Strikingly however, IFN α -treated adipocytes expressed drastically lower levels of UCP1 at the mRNA and protein level (Fig 3C and D) with no change in PRDM16 protein levels (Fig EV3A). IFN α treatment also decreased the expression of the brown fat marker gene *Cidea* and several mitochondrial genes, including *Cox7a1* and mitochondrial-encoded genes *mt-Cytb* and *mt-Co1* (Fig 3D). Pre-treatment of cells with α IFNAR prevented the decrease in *Ucp1* and *mt-Cytb* expression in mature adipocytes (Fig EV3B), confirming that the inhibitory effect of IFN α on brown fat and mitochondrial programming was due to elevated canonical IFN signaling. IFN α treatment similarly inhibited the beige fat program in inguinal adipocytes, including reducing the basal levels of mitochondrial genes and repressing (by ~50-fold) the rosi-stimulated expression of *Ucp1* (Fig EV3C).

We found that IFN treatment early in brown fat differentiation (day 0–4) led to a permanent reduction in the expression of brown fat and mitochondrial genes in mature adipocytes (5 days later); this included a ~60% reduction in *Ucp1* levels (Fig EV3D). By contrast, IFN α treatment during later stages (days 5–9) had less of an impact on the brown fat gene program, including a ~35% reduction in *Ucp1* and no significant change in *Cidea* expression. Overall, these results show that activation of the type I IFN system in brown preadipocytes and during early stages of differentiation specifically impairs the activation of brown fat-specific genes.

IFN α reduced the expression of specific mitochondrial proteins in brown fat cells, including MT-CO1, a subunit of complex IV, without affecting the levels of other mitochondrial components (Fig 3E). Control and IFN α -treated cells had comparable amounts of mitochondria DNA (Fig 3F), suggesting that IFN α treatment does not reduce mitochondrial biogenesis *per se*. However, transmission electron microscopic analyses revealed that IFN α treatment had profound effects on mitochondrial morphology. The mitochondria in control brown adipocytes contained dense and well-organized cristae whereas the mitochondria in IFN α -treated adipocytes had severely disorganized cristae with a highly reticular morphology (Fig 3G). Consistent with these morphological effects on mitochondria, IFN α -treated adipocytes displayed a 40% reduction in oxygen consumption as compared to control adipocyte cultures (Fig 3H).

To determine whether increased PRDM16 expression can protect brown fat cells against the inhibitory effects of exogenous IFN α , we transduced brown preadipocytes with control or PRDM16-expressing retroviral vectors and induced the cells to differentiate in the presence of IFN α or vehicle control. Remarkably, PRDM16 expression completely rescued *Ucp1* expression in IFN α -treated adipocytes. PRDM16 also mitigated the inhibitory effects of IFN α on the expression of *Cidea* and mitochondrial genes (*Cox7a1*, *mt-Cytb*) (Fig 3I). Taken together, these results demonstrate that type I IFN signaling suppresses mitochondrial function and decreases the thermogenic capacity of brown and beige adipocytes and this effect can be blocked by elevating PRDM16 levels.

PRDM16 opposes type I IFN signaling *in vivo*

An important question is whether PRDM16 regulates the response of BAT to type I IFN *in vivo*. To address this question, we treated 6- to 7-week-old BAT-selective *Prdm16* KO (KO) (*Myf5^{Cre}*; *Prdm16^{fllox}*) and littermate control mice with either vehicle or recombinant IFN α over a 2-week period. At this young age, ISGs are expressed at similar levels in control and KO BAT (Fig EV1C). However, the IFN α treatment of mice induced STAT1 protein to much higher levels in KO BAT than in WT BAT (Fig 4A). Furthermore, the mRNA levels of *Stat1* and several other ISGs were increased by IFN α treatment only in KO BAT (Figs 4B and EV4A). ISGs were expressed at comparable levels in the ingWAT of WT and BAT-selective *Prdm16* KO mice (Fig EV4C).

IFN α treatment had little impact on the morphology of BAT from control mice. Under basal conditions, the KO BAT had larger lipid droplets and reduced *Ucp1* gene levels (Fig 4C and D). The loss of brown fat character in KO BAT was exacerbated by IFN α treatment. This included diminished expression of UCP1 and brown fat-selective genes in BAT from IFN α -treated relative to control-treated KO animals (Figs 4C and D, and EV4B). Hematoxylin and eosin (H&E) staining of BAT sections revealed that there was greater lipid accumulation in the BAT of IFN α -treated KO mice relative to that in saline-treated KO mice (Fig 4C). In the ingWAT, where basal PRDM16 expression is low, the IFN treatment caused equivalent reduction in mitochondrial-encoded genes (*mt-Co1*, *mt-Cytb*) in both WT and KO mice.

We studied the effect of IFN α treatment on the thermogenic capacity of WT and BAT-selective *Prdm16* KO mice by measuring oxygen consumption (respiration) using metabolic cages. To

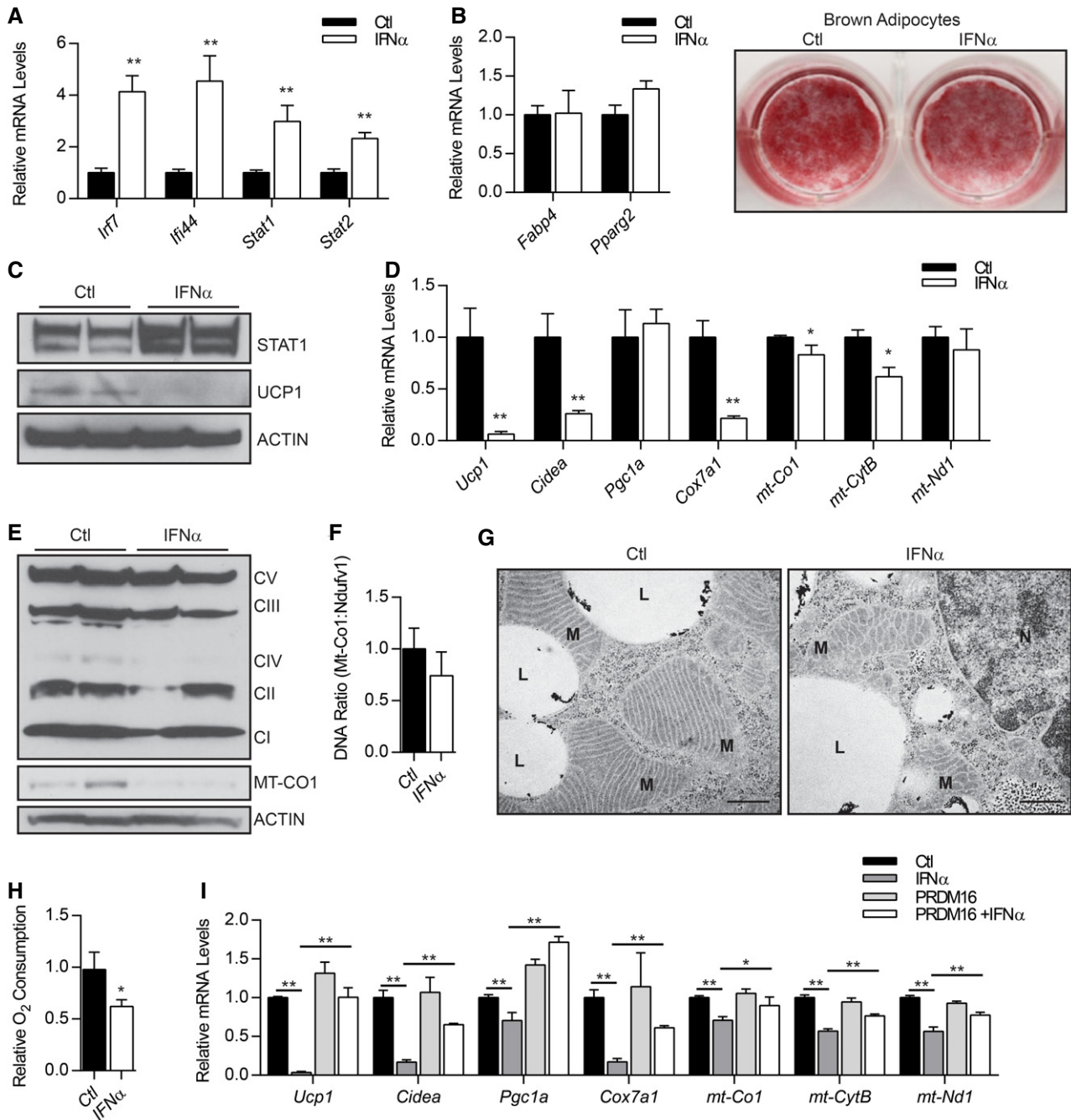


Figure 3. Type I IFN disrupts mitochondrial structure and function in adipocytes.

Brown adipocytes were treated with 1,000 U/ml mouse IFN α or vehicle (Ctl) throughout differentiation.

A Relative expression levels of ISGs. Data represent ($n = 3$) mean \pm standard deviation. ** $P \leq 0.01$ (Student's t -test).

B Oil Red O staining of lipid droplets and relative mRNA levels of pan-adipogenic genes (*Fabp4*, *Pparg2*). Data represent ($n = 3$) mean \pm standard deviation.

C Western blot analysis of STAT1, UCP1, and actin (loading control) protein levels.

D Relative mRNA levels of brown fat-selective (*Ucp1*, *Cidea*, *Pgc1a*) and mitochondrial (*Cox7a1*, *mt-Co1*, *mt-Cytb*, *mt-Nd1*) genes. Data represent ($n = 3$) mean \pm standard deviation and are consistent with duplicate independent experiments. * $P \leq 0.05$, ** $P \leq 0.01$ (Student's t -test).

E Western blot analysis of mitochondrial complex proteins and actin (loading control).

F Relative ratio of mitochondrial DNA (mt-Co1) to nuclear DNA (Ndufv1) ($n = 6$). Data are presented as mean \pm standard deviation.

G Transmission electron micrograph of representative brown adipocytes showing mitochondria (M), lipid droplets (L), and nuclei (N). Scale bar = 500 nm.

H Relative oxygen consumption rates of adipocytes ($n = 6$). Data are presented as mean \pm standard deviation. * $P \leq 0.05$ (Student's t -test).

I Relative mRNA levels of brown-selective genes (*Ucp1*, *Cidea*, *Pgc1a*) and mitochondrial genes (*mt-Co1*, *mt-Cytb*, *mt-Nd1*) in brown adipocytes infected with control (Ctl) or PRDM16 retrovirus +/- mouse IFN α . Data represent ($n = 3$) mean \pm standard deviation. * $P \leq 0.05$, ** $P \leq 0.01$ (paired two-way ANOVA).

Source data are available online for this figure.

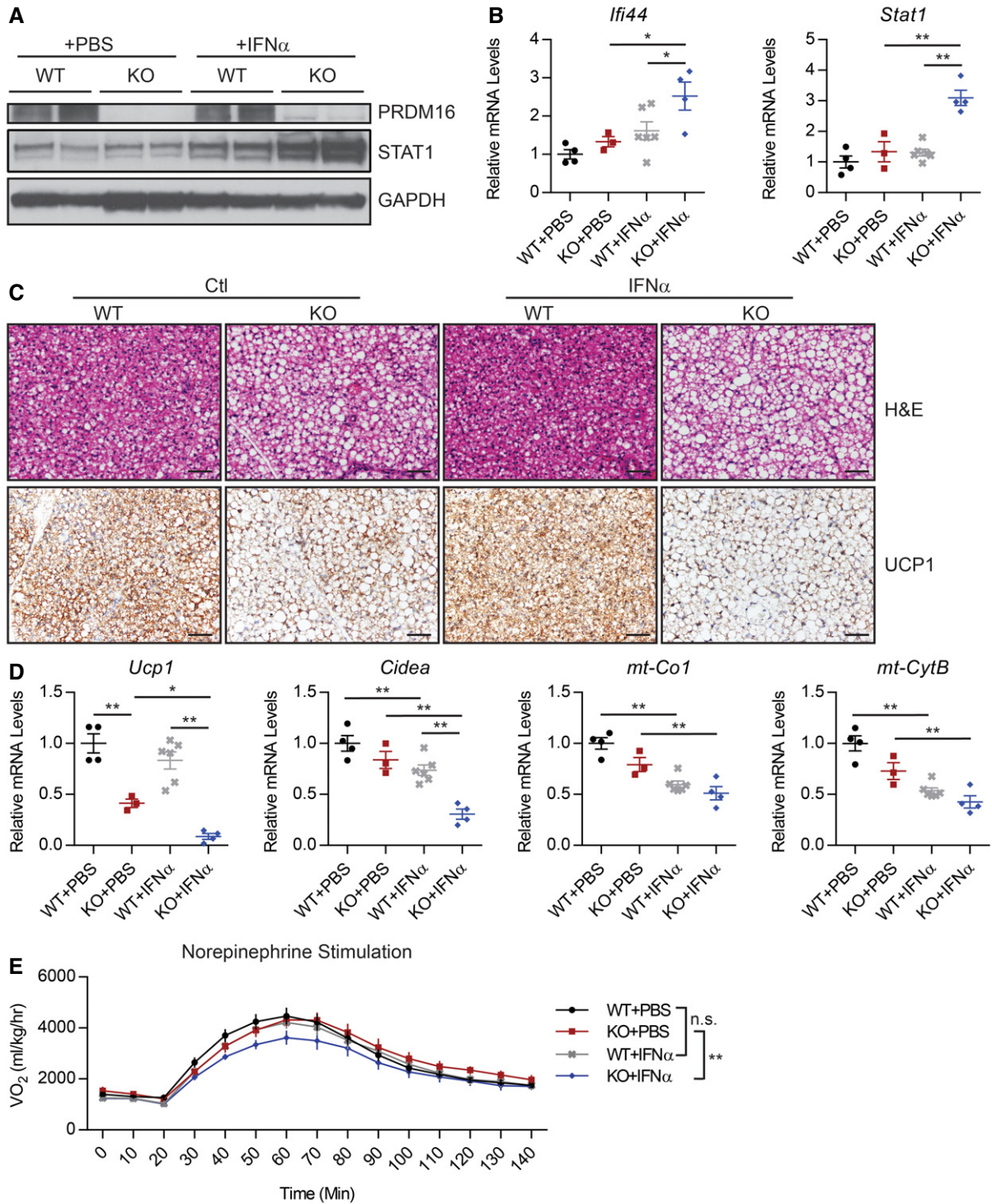


Figure 4. PRDM16 opposes type I IFN signaling in vivo.

A–D *Prdm16*^{fl/fl} (WT) and *Myf5*^{Cre}; *Prdm16*^{fl/fl} (KO) mice treated with IFN α or phosphate-buffered saline (PBS) for 2 weeks prior to analysis of brown adipose tissue (BAT). Experimental groups: WT+PBS ($n = 4$), KO+PBS ($n = 3$), WT+IFN ($n = 6$), KO+IFN ($n = 4$). (A) Western blot analysis of PRDM16, STAT1, and GAPDH (loading control) protein levels. (B) qPCR analysis of *Ifi44* and *Stat1* mRNA levels. Data are presented as mean \pm SEM. * $P \leq 0.05$, ** $P \leq 0.01$ (paired two-way ANOVA). (C) Hematoxylin and eosin (H&E) and anti-UCP1 immunohistochemical staining. Scale bar = 50 μ m. (D) Relative mRNA levels of brown fat-specific genes (*Ucp1*, *Cidea*) and mitochondrial genes (*mt-Co1*, *mt-CytB*). Data are presented as mean \pm SEM. * $P \leq 0.05$, ** $P \leq 0.01$ (paired two-way ANOVA).

E Volume of O₂ (VO₂) consumed before and after norepinephrine injection. Experimental groups: WT+PBS ($n = 9$), KO+PBS ($n = 6$), WT+IFN ($n = 6$), KO+IFN ($n = 7$). Data are presented as mean \pm SEM. ** $P \leq 0.01$ (paired two-way ANOVA).

Source data are available online for this figure.

specifically evaluate BAT activity, we monitored respiration in anesthetized mice before and after stimulation with norepinephrine (NE), the physiological inducer of brown fat thermogenesis. Interestingly, there was no significant difference in NE-stimulated respiration between WT (control) mice treated with vehicle or IFN α . However, KO mice treated with IFN α displayed a significant reduction in NE-induced respiration compared to vehicle-treated KO mice ($P = 0.002$) (Fig 3E). These results suggest that the PRDM16-mediated suppression of type I IFN responses is required for preserving BAT function.

PRDM16 represses ISG transcription through direct binding at promoter/enhancers

PRDM16 is a transcriptional factor that binds at brown fat-selective gene enhancers to activate gene transcription. Chromatin immunoprecipitation combined with high-throughput sequencing (ChIP-seq) in brown preadipocytes showed that PRDM16 also binds at or near the promoter regions of many ISGs, including *Ifi44* and *Oas3* (Fig 5A). These PRDM16-bound regions had lower levels of the activating histone mark H3K27 acetylation in PRDM16-expressing cells, suggesting that they are functional sites (Fig 5A). ChIP-qPCR experiments confirmed that PRDM16 binds proximal to many of the ISGs that are reduced in expression by PRDM16 (Fig 5B).

PRDM16 has several domains, including an N-terminal PR domain with methyltransferase function, two zinc-finger clusters (ZF1 and ZF2) that can bind to DNA, and a transcriptional repressor domain that interacts with C-terminal binding proteins (CtBPs) (Nishikata *et al*, 2003; Ishibashi & Seale, 2015). To investigate which, if any, of these PRDM16 domains/activities are critical for ISG repression, we expressed mutant forms of PRDM16 in *Prdm16* KO brown preadipose cells. PRDM16 mutants that lack CtBP-binding or methyltransferase activity (e.g. PR-domain mutant) repressed the expression of STAT1 and other ISGs to a similar degree as wild-type PRDM16 (Fig 5C and D). However, a DNA-binding mutant form of PRDM16 harboring a point mutation in the second zinc-finger cluster (R998Q) had almost no capacity to repress ISGs (Fig 5C and D), though it activates brown fat genes and represses white fat genes normally (Fig EV5A and B, and Seale *et al*, 2007). These results suggest that DNA-binding is critical for PRDM16-mediated suppression of ISGs, but not for activation of brown fat-selective genes.

PRDM16 blocks the activation of ISGs by IRF1

We identified an overlapping IFN-stimulated response element (ISRE) and IRF-binding element (IRF-E) at many of PRDM16 binding sites at ISG promoters, including at the *Ifi44* promoter (Fig EV6A). IFN regulatory factors (IRFs) are critical transcriptional effectors of the IFN signaling circuitry (Fujita *et al*, 1989; Harada *et al*, 1990; Kimura *et al*, 1994; Schafer *et al*, 1998; Sato *et al*, 2000). Moreover, various IRFs have been shown to regulate adipocyte differentiation and function (Eguchi *et al*, 2008, 2011; Kong *et al*, 2014; Kumari *et al*, 2016). Among the IRF family members, we found that *Irf1* and *Irf7* were particularly highly expressed in brown preadipocytes (Fig EV6B). IRF1 was a prime candidate for further study because it is known to activate a similar ISG signature as IFN α , including STAT1 (Xu *et al*, 2016). IRF1 expression levels are relatively

constant throughout the process of adipocyte differentiation (Fig EV6C). To test whether IRF1 was required for ISG induction in *Prdm16*-deficient brown adipocytes, we used lentiviral delivery of short-hairpin RNAs (shRNAs) to knock down *Irf1* expression. Two shRNA sequences were effective in reducing IRF1 protein levels and resulted in 50–70% reductions in the expression of many ISGs, including *Irf7*, *Ifi44*, and *Stat1* (Fig 6A and B). The shRNA-mediated reduction in ISG expression was reversed by co-expression of the shRNA-resistant human form of IRF1 (Fig EV6D). CRISPR/Cas9-mediated reduction in IRF1 in *Prdm16*-deficient brown adipocytes also decreased ISG expression (Fig EV6F). In mature brown adipocytes with endogenous levels of *Prdm16* expression, knock-down of *Irf1* did not affect ISG or brown fat gene expression (Fig EV6E), whereas ectopic IRF1 expression in fibroblasts increased ISG levels (Fig 6C and D).

We then explored whether PRDM16 functionally interacts with IRF1 to regulate ISG expression. We used the proximal *Ifi44* promoter, containing an identified PRDM16-binding site (Fig EV6A), to drive expression of a *Luciferase* reporter. IRF1 robustly activated the *Ifi44* promoter, and this induction was very effectively blocked by co-expression of WT but not the R998Q mutant form of PRDM16 (Fig 6E). We were unable to detect any evidence of a physical interaction between IRF1 and PRDM16 using a variety of approaches, and PRDM16 expression did not change IRF1 levels (Fig EV6G and H). Furthermore, PRDM16 did not repress the activating function of a GAL4 DBD (DNA-binding domain)-IRF1 fusion protein on a *Gal4 DBD*-driven reporter (Fig EV6I). These results suggest that PRDM16 does not repress IRF1 function through physical binding and that the repressive effect of PRDM16 requires the IRF-binding site and/or other nearby promoter elements.

PRDM16 suppressed IRF1-mediated gene activation in a dose-dependent manner (Fig 6F), suggesting that PRDM16 may compete with IRF1 for binding to the *Ifi44* promoter. Consistent with this, the isolated IRF-E/ISRE site alone was sufficient to confer responsiveness to both IRF1 and PRDM16 in transcription assays (Fig 6G). Additionally, we found that PRDM16 expression decreased IRF1 binding at several native ISG promoters using ChIP-qPCR (Fig 6H). Finally, in WT brown preadipocytes with endogenous PRDM16 levels, recombinant IFN α increased IRF1 binding to various ISGs, while *Prdm16* KO cells displayed higher IRF1 binding (Fig EV6J). Together, these results suggest that PRDM16 represses ISG target genes by binding to IRF elements and blocking access to the transcriptional activator, IRF1 (Fig 6I).

Discussion

PRDM16 is a critical transcriptional regulator of brown and beige adipocyte identity. PRDM16 co-regulates other DNA-binding factors to promote the transcription of brown fat genes in adipocytes (Seale *et al*, 2007, 2008; Kajimura *et al*, 2009). We show here that, in addition to its direct transcriptional activating effect on brown fat-specific genes, PRDM16 reinforces and maintains brown fat identity by suppressing the type I IFN response. PRDM16 blocks the activation of IFN-induced genes by competing with IRF1 for binding to IRF-E binding motifs. While the interaction between PRDM16 and IRF1 plays an important role in regulating the IFN response in

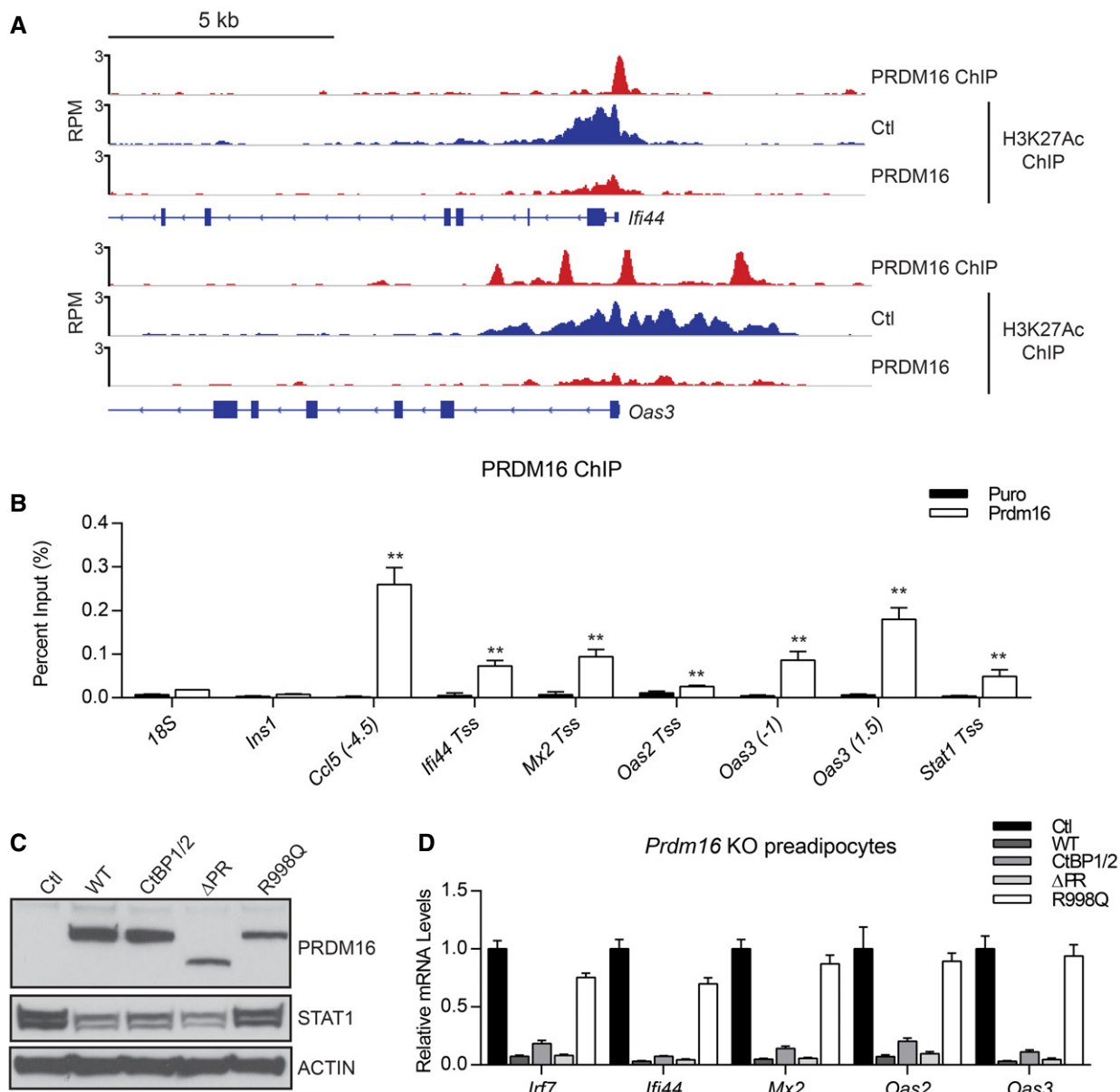


Figure 5. PRDM16 represses ISGs through direct binding at gene promoters.

A ChIP-seq stack-height profiles in reads per million (RPM) for PRDM16 and H3K27 acetylation (Ac) at *Ifi44* and *Oas3* in *Prdm16* KO brown adipocyte precursors that express PRDM16 or a control (Ctl) retrovirus.

B ChIP-qPCR analysis of PRDM16 binding at ISG promoters/enhancers in control (Ctl) or PRDM16-expressing brown preadipose cells. *Ins1* and *18S* were used as non-specific binding site controls. Data represent ($n = 3$) mean \pm standard deviation and are consistent with results from duplicate independent experiments. $**P \leq 0.01$ (Student's *t*-test).

C Western blot analysis of STAT1 and PRDM16 protein levels in *Prdm16* KO brown preadipose cells transduced with retroviral vectors that express different forms of PRDM16: wild-type (WT), CtBP-binding mutant (CtBP1/2), PR-domain deletion mutant (Δ PR), DNA-binding mutant (R998Q), or empty vector (Ctl). Loading control, actin.

D Relative mRNA levels of ISGs in cells from (C). Data represent ($n = 3$) mean \pm standard deviation.

Source data are available online for this figure.

adipogenic cells, whether PRDM16 also functionally interacts with other IRFs remains to be determined. Notably, PRDM1, a related family member, also binds to the IRF1-binding element to repress activation of the IFN pathway in other cell types (Kuo & Calame, 2004; Doody *et al*, 2007; Mould *et al*, 2015), suggesting that

PRDM16 and PRDM1 may have overlapping roles in regulating the type I IFN pathway.

Type I IFNs are best known for their role in mounting antiviral responses. Virus-infected cells secrete and respond to type I IFNs, including IFN α and IFN β . These cytokines establish an antiviral

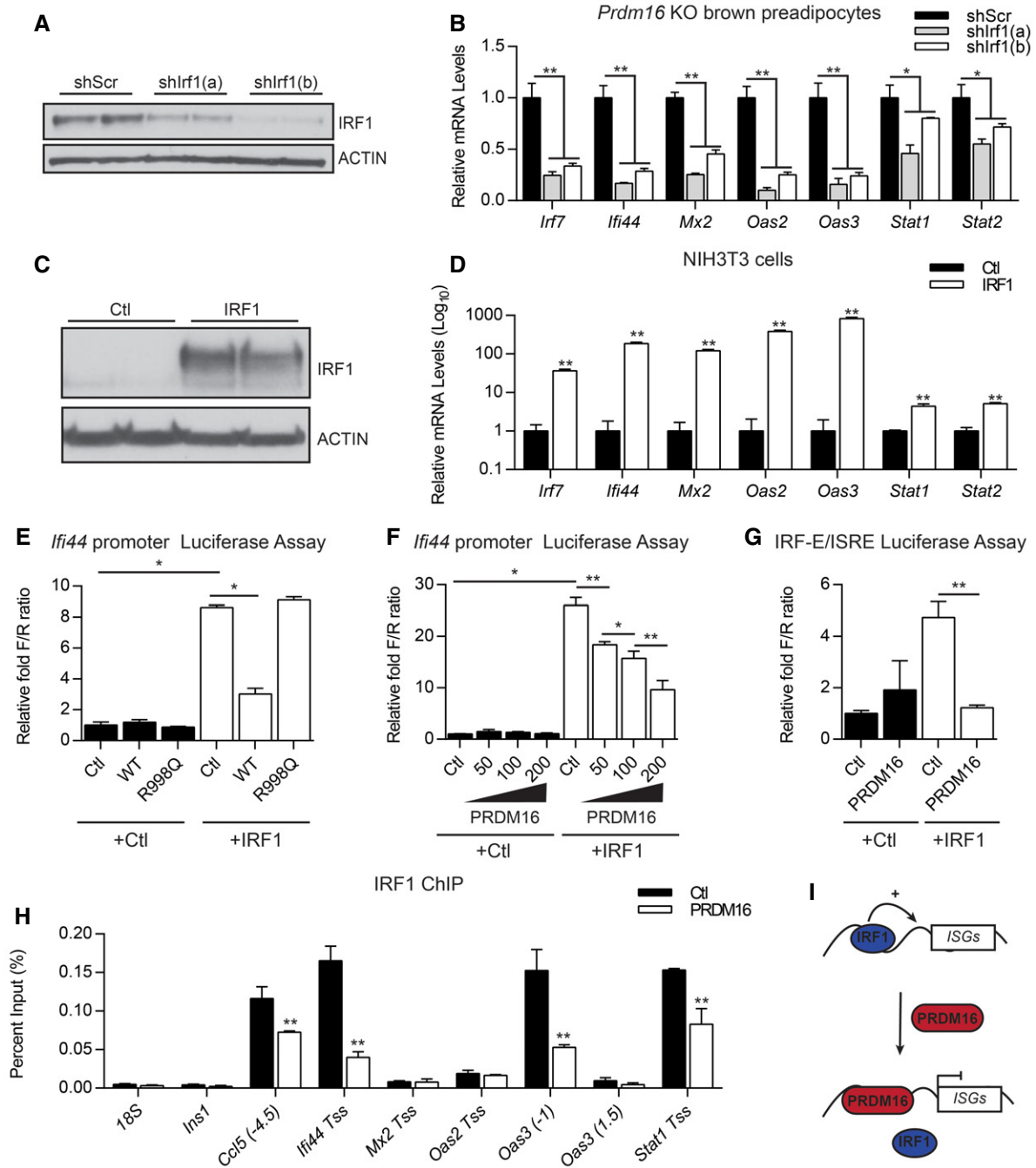


Figure 6. PRDM16 blocks the activation of ISGs by IRF1.

A, B Western blot analysis of IRF1 and actin (loading control) protein levels (A) and relative mRNA levels of ISGs (B) in *Prdm16* KO brown preadipocytes transduced with lentiviral short-hairpin RNA directed against *Irf1* (shIrf1a, shIrf1b) or a scrambled control (shScr).

C, D Western blot analysis of IRF1 and actin (loading control) protein levels (C) and relative mRNA levels of ISGs (D) in cells from NIH3T3 cells transfected with CMV6 (Ctl) or CMV6-IRF1.

E Transcriptional activity of the *Irf44* promoter in NIH3T3 cells upon expression of IRF1 and wild-type (WT) or DNA-binding mutant (R998Q) forms of PRDM16.

F Transcriptional activity of the *Irf44* promoter in response to IRF1 expression and increasing amounts of PRDM16 expression.

G Transcriptional activity of the IFN regulatory factor-binding element (IRF-E)/IFN-stimulated response element (ISRE) in *Irf44* in response to IRF1 and/or PRDM16.

H ChIP-qPCR analysis of IRF1 binding at ISGs in brown preadipocytes transduced with PRDM16 or control (Ctl) retrovirus. *Ins1* and *18S* were used as non-specific binding site controls.

I Proposed model for PRDM16-action at ISG promoter regions.

Data information: Data represent ($n = 3$) mean \pm standard deviation (B, D) and ($n = 3$) mean \pm SEM (E–H) and are consistent with results from duplicate independent experiments. * $P \leq 0.05$, ** $P \leq 0.01$ (Student's t -test).

Source data are available online for this figure.

state through multiple mechanisms, including the production of antimicrobial proteins that act directly on viruses and modulation of the adaptive immune response (Honda *et al*, 2005). The importance of this pathway is underscored by the finding that mice lacking the type I IFN receptor (IFNAR) rapidly succumb to viral infections (Hwang *et al*, 1995). Similarly, humans with mutations in STAT1, a key effector of the IFN response, die from viral infection (Dupuis *et al*, 2003; Chappier *et al*, 2006). The suppressive effect of PRDM16 on IFN responses may be important for preserving the thermogenic function of BAT in virus-infected animals. This may be especially important in small animals such as newborns to survive cold exposure while dealing with viral infection. PRDM16 may also be needed to protect BAT activity during viral infection in order to support hyperthermia (fever).

Low levels of type I IFN, particularly IFN β , are also present in many cells/tissues in the absence of infection (Tovey *et al*, 1987; Hamilton *et al*, 1996; Hida *et al*, 2000; Hata *et al*, 2001; Abt *et al*, 2012). Constitutive type I IFN expression is believed to be a priming mechanism for rapid induction of the pathway upon viral infection (Vogel & Fertsch, 1984; Hata *et al*, 2001; Abt *et al*, 2012; Ganai *et al*, 2012; Kawashima *et al*, 2013). Similarly, increased type I IFN signaling can increase cellular responsiveness to other cytokines, such as IFN γ by increasing the levels of common signaling intermediates like STAT1 (Hamilton *et al*, 1996; Gough *et al*, 2010). Interestingly, the type I IFN pathway is required to achieve the proper balance of proliferation and maturation of hematopoietic stem cells (HSCs) (Essers *et al*, 2009; Kim *et al*, 2016). In this context, elevated IFN signaling leads to stem cell exhaustion (Essers *et al*, 2009; Sato *et al*, 2009), highlighting the importance of a tightly regulated IFN system. Notably, PRDM16 is also a critical regulator of HSCs (Chukov *et al*, 2010), suggesting that regulation of IFN signaling may be a key function of PRDM16 in this compartment. Along these lines, it will now be important to determine whether the PRDM16 and IFN regulate the proliferation and/or maintenance of brown adipose precursors.

A prominent effect of IFN activation in brown adipocytes is reduced mitochondrial function and abnormal mitochondrial morphology (Fig 3). This result agrees with previous studies showing that IFN α inhibits the expression of mitochondrial-encoded genes in lymphoid cells (Shan *et al*, 1990; Lewis *et al*, 1996). We found that IFN α activation leads to a loss of cristae structure and a reduction in specific mitochondrial proteins like MT-CO1 in brown adipocytes. The mechanism(s) by which IFN activation reduces mitochondrial function is unclear. One possibility is that IFN-activated STAT1/2 directly represses the transcription of *Ucp1* and mitochondrial-encoded genes. However, type I IFN induces a large number of downstream ISGs, any of which could have as yet undetermined roles in regulating mitochondrial function and cellular metabolism. Importantly, blocking JAK-STAT signaling in human adipocytes decreases IFN signaling and induces brown fatlike characteristics (Moisan *et al*, 2015), suggesting a potentially important role for this pathway in human metabolism.

In summary, PRDM16 regulates the brown fat gene program through multiple mechanisms, including via direct actions at brown fat gene enhancers and indirectly by suppressing the type I IFN-driven gene program. Our study also suggests potentially important links between innate immune and metabolic pathways in

adipocytes that warrant further investigation and predicts a potential role for IFN signaling in metabolic regulation. In support of this, genetic manipulations that influence the type I IFN pathway in mice have revealed significant metabolic phenotypes. For example, IRF3 knockout mice have increased energy expenditure due to the browning of the inguinal adipose (Kumari *et al*, 2016). Moreover, both IRF7 and IRF3 knockout mice are protected from diet-induced obesity and have improved insulin sensitivity (Wang *et al*, 2013; Kumari *et al*, 2016). Additional focus on the role of type I IFN in adipocytes may reveal new approaches to preserve and/or increase brown fat activity for the treatment of obesity and metabolic disease.

Materials and Methods

Animals

All animal experiments were approved by the University of Pennsylvania's Institutional Animal Care and Use Committee. *Rosa26^{CreER}*, *Prdm16^{flox}* mice were maintained on a mixed 129Sv/C57Black6 genetic background (Harms *et al*, 2014). *Myf5^{Cre}*; *Prdm16^{flox}* mice were backcrossed into the C57Black6 background for 10 generations (Harms *et al*, 2014). Male mice were used for all experiments. Mice (6–7 weeks old) were injected with 25,000 U of recombinant mouse interferon alpha A (PBL Assay Science) or an equal volume of phosphate-buffered saline (PBS) as control six times over 2 weeks. For NE injections, mice were first placed in CLAMS metabolic chambers at 33°C, then sedated with 75 mg/kg Nembutal, followed 20 min later by injection with 1 mg/kg NE (Sigma A9512-1G). Data were collected until mice recovered from barbiturate sedation.

Cell culture

Primary inguinal preadipocytes were isolated from *Prdm16^{flox}* and *Rosa26^{CreER}*, *Prdm16^{flox}* mice as previously described (Rajakumari *et al*, 2013). Recombination in *Rosa26^{CreER}*, *Prdm16^{flox}* adipocytes was induced by treating cells with 1 μ M of 4-hydroxy-tamoxifen (Sigma) for 3 days in growth phase. Cells were differentiated with medium containing 10% FBS, 0.5 μ M isobutylmethylxanthine, 125 nM indomethacin, 1 μ M dexamethasone, 20 nM insulin, and 1 nM T3 without or with 1 μ M rosiglitazone. To block type I IFN signaling, cells were treated with 1 μ g/ml anti-IFNAR1 antibody MAR1-5A3 (Leinco Technologies, Inc.) during growth for 4 days. Immortalized brown and primary ingWAT adipocytes were treated with vehicle or 1,000 U/ml recombinant mouse interferon alpha A (PBL Assay Science) throughout differentiation to determine effects of IFN on differentiation. For CRISPR/Cas9-mediated gene editing, guide RNA sequences against mouse *Prdm16* were cloned into LentiCRISPR (Shalem *et al*, 2014), a gift from Feng Zhang (Addgene, 49535). A guide targeted at the mouse *Rosa26* locus was used as a negative control. gRNA-*Prdm16*(A): 5' CGGCGTCATCCGCTGTGTC 3'; gRNA-*Prdm16*(B): 5' CCAACCTGTGCCGGCACAAG 3'; gRNA-R26: 5' AAGATGGGCGGAGTCTTCT 3'; gRNA-Irf1(A): 5' AGCAGCTGCTAAGCACGGC 3'; gRNA-Irf1(B): 5' GCACGCTGCTAAGCACGCT 3'. Short-hairpin RNA (shRNA) constructs were generated by the High-Throughput Screening Core (University of Pennsylvania).

shIrf1(a): 5' AGATGGACATTATACCAGATA 3'; shIrf1(b): 5' CTCTTCTGTCTATGGAGACTT 3'. Oil Red O staining and retrovirus production were performed as described previously (Seale *et al*, 2007).

Real-time qPCR

Total RNA was extracted by TRIzol (Invitrogen) followed by purification using PureLink RNA columns (Invitrogen). Isolated mRNA was reverse transcribed using the High-Capacity cDNA Synthesis kit (Applied Biosystems) and used in real-time qPCRs with SYBR Green master mix (Applied Biosystems) on a 7900 HT (Applied Biosystems). TATA-binding protein (*Tbp*) was used as an internal normalization control.

Microarray data

Microarray services were provided by the UPENN Molecular Profiling Facility, including quality control tests of the total RNA samples by Agilent Bioanalyzer and Nanodrop spectrophotometry. All protocols were conducted as described in the Ambion Expression Manual and the Affymetrix GeneChip Expression Analysis Technical Manual. In microarray data of control (EtOH) and *Prdm16* KO (4OHT) cells under control (Ctl) or rosiglitazone (*rosi*) (GSE86018), differentially expressed genes were selected for clustering analysis by fold change > 1.5 and adjusted *P*-value < 0.05. Hierarchical clustering was performed using (1–Spearman correlation coefficient) as a distance measure for genes and samples. Gene ontology analysis was conducted using Enrichr (Chen *et al*, 2013; Kuleshov *et al*, 2016), and top enriched biological process terms were presented. For *Prdm16* KO BAT gene expression data, we used previously published microarray data (Harms *et al*, 2014, 2015).

Cell immunostaining

Briefly, cells were fixed with 4% (wt/vol) paraformaldehyde (PFA) for 10 min, permeabilized with 0.5% Triton X-100 for 15 min, and then blocked in 4% goat serum for 30 min. Cells were then incubated with primary antibody anti-Prdm16 1:200 (Seale *et al*, 2007), followed by secondary antibody Alexa Fluor 647 donkey anti-rabbit IgG 1:500 (Invitrogen), and DAPI (Invitrogen) for nuclear staining.

Western blot

Protein extracts were prepared as previously described (Rajakumari *et al*, 2013). Proteins were separated in 4–12% Bis–Tris NuPAGE gels (Invitrogen) and transferred to PVDF membranes. For Western blot, antibodies used were as follows: anti-PRDM16 (Seale *et al*, 2007), anti-FLAG (Sigma, F1804), anti-pSTAT1 (Santa Cruz, sc7988), anti-STAT1 (Santa Cruz, sc-346), anti-pSTAT2 (Millipore, 07-224), anti-STAT2 (Cell Signaling Technology, 4597S), anti-STAT3 (Cell Signaling Technology, 9139S), anti-tubulin (Sigma, T6199), anti-UCP1 (R&D Systems, MAB6158), anti-actin (Millipore), total OXPHOS antibody cocktail (Abcam, ab110413), anti-MT-CO1 (Abcam, ab14705), and anti-IRF1 (Cell Signaling Technology, 8478S).

Chromatin immunoprecipitation

Immortalized brown preadipocytes infected with MSCV–Puromycin or MSCV–Prdm16 were grown to confluency and fixed in 1% formaldehyde for 15 min, then quenched with 125 mM glycine for 5 min. ChIP was performed as described previously (Harms *et al*, 2015). Chromatin was probed with 1 μg of the following antibodies: anti-PRDM16 (Harms *et al*, 2014) or anti-histone H3K27Ac (Abcam, ab4729). Bound fragments were eluted at 65°C overnight in 20 mM Tris pH 8, 1 mM EDTA, and 1% SDS and subsequently treated with RNaseA and proteinase K before undergoing column purification (Qiagen, 28104). Target enrichment was calculated as percent input. ChIP-seq reads for Prdm16 and H3K27Ac (GSE86017) were aligned to mouse genome, mm9, and further processed for peak-calling and genome browser track creation as previously described (Harms *et al*, 2015).

Tissue O₂ consumption

Differentiated brown adipocytes were trypsinized, pelleted, and resuspended in a buffer comprised of 2% BSA, 1.1 mM sodium pyruvate, and 25 mM glucose in PBS. Samples were placed in an MT200A Respirometer Cell (Strathkelvin), and oxygen consumption was measured for ~5 min. Oxygen consumption was normalized to total cell number.

Histology

For immunohistochemistry, BAT was fixed in 4% PFA overnight, dehydrated, and embedded in paraffin for sectioning. Sections were stained with hematoxylin and eosin or probed with antibodies for UCP1 (R&D Systems). For transmission electron microscopy, adipocytes were fixed with 2.5% glutaraldehyde, 2.0% paraformaldehyde in 0.1 M sodium cacodylate buffer (pH 7.4) overnight at 4°C, and then post-fixed with 2.0% osmium tetroxide for 1 h at room temperature. Thin sections were stained with uranyl acetate and lead citrate and examined with a JEOL 1010 electron microscope.

Transcription assays

The *Ifi44* promoter/luciferase reporter plasmid (pGL4-*Ifi44*p) was constructed by PCR cloning of genomic sequence from C57Bl/6 DNA corresponding to 441 bp of *Ifi44* proximal promoter and 76-bp 5' UTR into the XhoI and NcoI sites of pGL4.24, replacing the existing minimal promoter (Promega). pGL4-*Ifi44*p-ISRE (IRF-E/ISRE) was built by inserting a 55-bp linker centered at the *Ifi44* transcriptional start site (and ISRE) into the KpnI and XhoI sites of pGL4.24, retaining the minimal promoter. CMX-Gal4(DBD)-hIRF1 was cloned by PCR amplifying human IRF1 from CMV6-hIRF1, with BamHI and NotI sites appended for insertion into CMX-Gal4(DBD). pRL-CMV was used for internal normalization of the dual luciferase assays. The CMX-Gal4(DBD) (containing 447 bp of the Gal4 DNA-binding domain), Gal4(5x)SV40-Luc, and pRL-CMV plasmids were provided by Mitch Lazar (University of Pennsylvania). CMX-hIRF1 was provided by Kathleen Sullivan (Children's Hospital of Pennsylvania). Reporter and expression plasmids were co-transfected into NIH3T3 cells (ATCC) using Lipofectamine 2000 (Invitrogen);

11668019). At 48 h post-transfection, cells were harvested into passive lysis buffer for dual luciferase assays (Promega; E1960) using a Synergy HT plate reader (BioTek).

Statistical analysis

Energy expenditure data were analyzed in R using a paired three-way ANOVA over all time points after NE injection with significance level, $\alpha = 0.05$. Subsequent paired two-way ANOVAs for treatment effects over all time points were performed in individual genotype arms if interaction terms were significant at $\alpha = 0.05$.

Expanded View for this article is available online.

Acknowledgements

We would like to thank the Histology and Gene Expression Core of the Penn Cardiovascular Institute for immunohistochemistry; the Electron Microscopy Core for processing and imaging; the UPENN Molecular Profiling Facility for microarray services; and the Functional Genomics Core of the Penn Diabetes and Endocrinology Center (DK19525) for ChIP sequencing. This work was funded by NIH/NIDDK grants R01DK103008 and R01DK107589 (P. Seale).

Author contributions

MK, JI, and MJH performed the experiments shown here. H-WL and K-JW analyzed microarray and ChIP-Seq data. RRS provided advice on experimental setup and project development. MK and PS conceived the experiments and wrote the manuscript.

Conflict of interest

The authors declare that they have no conflict of interest.

References

- Abt MC, Osborne LC, Monticelli LA, Doering TA, Alenghat T, Sonnenberg GF, Paley MA, Antenus M, Williams KL, Erikson J, Wherry EJ, Artis D (2012) Commensal bacteria calibrate the activation threshold of innate antiviral immunity. *Immunity* 37: 158–170
- Aguilo F, Avagyan S, Labar A, Sevilla A, Lee DF, Kumar P, Lemischka IR, Zhou BY, Snoeck HW (2011) Prdm16 is a physiologic regulator of hematopoietic stem cells. *Blood* 117: 5057–5066
- Auffret J, Viengchareun S, Carre N, Denis RG, Magnan C, Marie PY, Muscat A, Feve B, Lombes M, Binart N (2012) Beige differentiation of adipose depots in mice lacking prolactin receptor protects against high-fat-diet-induced obesity. *FASEB J* 26: 3728–3737
- Bromberg JF, Horvath CM, Wen Z, Schreiber RD, Darnell JE Jr (1996) Transcriptionally active Stat1 is required for the antiproliferative effects of both interferon alpha and interferon gamma. *Proc Natl Acad Sci USA* 93: 7673–7678
- Cederberg A, Gronning LM, Ahren B, Tasken K, Carlsson P, Enerback S (2001) FOXO2 is a winged helix gene that counteracts obesity, hypertriglyceridemia, and diet-induced insulin resistance. *Cell* 106: 563–573
- Chappier A, Wynn RF, Jouanguy E, Filipe-Santos O, Zhang S, Feinberg J, Hawkins K, Casanova JL, Arkwright PD (2006) Human complete Stat-1 deficiency is associated with defective type I and II IFN responses *in vitro* but immunity to some low virulence viruses *in vivo*. *J Immunol* 176: 5078–5083
- Chen EY, Tan CM, Kou Y, Duan Q, Wang Z, Meirelles GV, Clark NR, Ma'ayan A (2013) Enrichr: interactive and collaborative HTML5 gene list enrichment analysis tool. *BMC Bioinformatics* 14: 128
- Chukov S, Levi BP, Smith ML, Morrison SJ (2010) Prdm16 promotes stem cell maintenance in multiple tissues, partly by regulating oxidative stress. *Nat Cell Biol* 12: 999–1006
- Cohen P, Levy JD, Zhang Y, Frontini A, Kolodin DP, Svensson KJ, Lo JC, Zeng X, Ye L, Khandekar MJ, Wu J, Gunawardana SC, Banks AS, Camporez JP, Jurczak MJ, Kajimura S, Piston DW, Mathis D, Cinti S, Shulman GI et al (2014) Ablation of PRDM16 and beige adipose causes metabolic dysfunction and a subcutaneous to visceral fat switch. *Cell* 156: 304–316
- Digby JE, Montague CT, Sewter CP, Sanders L, Wilkison WO, O'Rahilly S, Prins JB (1998) Thiazolidinedione exposure increases the expression of uncoupling protein 1 in cultured human preadipocytes. *Diabetes* 47: 138–141
- Doody GM, Stephenson S, McManamy C, Toozie RM (2007) PRDM1/BLIMP-1 modulates IFN-gamma-dependent control of the MHC class I antigen-processing and peptide-loading pathway. *J Immunol* 179: 7614–7623
- Dupuis S, Jouanguy E, Al-Hajjar S, Fieschi C, Al-Mohsen IZ, Al-Jumaah S, Yang K, Chappier A, Eidenschenk C, Eid P, Al Ghonaium A, Tufenkeji H, Frayha H, Al-Gazlan S, Al-Rayes H, Schreiber RD, Gresser I, Casanova JL (2003) Impaired response to interferon-alpha/beta and lethal viral disease in human STAT1 deficiency. *Nat Genet* 33: 388–391
- Eguchi J, Yan QW, Schones DE, Kamal M, Hsu CH, Zhang MQ, Crawford GE, Rosen ED (2008) Interferon regulatory factors are transcriptional regulators of adipogenesis. *Cell Metab* 7: 86–94
- Eguchi J, Wang X, Yu S, Kershaw EE, Chiu PC, Dushay J, Estall JL, Klein U, Maratos-Flier E, Rosen ED (2011) Transcriptional control of adipose lipid handling by IRF4. *Cell Metab* 13: 249–259
- Essers MA, Offner S, Blanco-Bose WE, Waibler Z, Kalinke U, Duchosal MA, Trumpp A (2009) IFNalpha activates dormant haematopoietic stem cells *in vivo*. *Nature* 458: 904–908
- Feldmann HM, Golozoubova V, Cannon B, Nedergaard J (2009) UCP1 ablation induces obesity and abolishes diet-induced thermogenesis in mice exempt from thermal stress by living at thermoneutrality. *Cell Metab* 9: 203–209
- Fujita T, Kimura Y, Miyamoto M, Barsoumian EL, Taniguchi T (1989) Induction of endogenous IFN-alpha and IFN-beta genes by a regulatory transcription factor, IRF-1. *Nature* 337: 270–272
- Ganal SC, Sanos SL, Kallfass C, Oberle J, Johner C, Kirschning C, Lienenklaus S, Weiss S, Staeheli P, Aichele P, Diefenbach A (2012) Priming of natural killer cells by nonmucosal mononuclear phagocytes requires instructive signals from commensal microbiota. *Immunity* 37: 171–186
- Gough DJ, Messina NL, Hii L, Gould JA, Sabapathy K, Robertson AP, Trapani JA, Levy DE, Hertzog PJ, Clarke CJ, Johnstone RW (2010) Functional crosstalk between type I and II interferon through the regulated expression of STAT1. *PLoS Biol* 8: e1000361
- Guerra C, Koza RA, Yamashita H, Walsh K, Kozak LP (1998) Emergence of brown adipocytes in white fat in mice is under genetic control. Effects on body weight and adiposity. *J Clin Invest* 102: 412–420
- Hamilton JA, Whitty GA, Kola I, Hertzog PJ (1996) Endogenous IFN-alpha beta suppresses colony-stimulating factor (CSF)-1-stimulated macrophage DNA synthesis and mediates inhibitory effects of lipopolysaccharide and TNF-alpha. *J Immunol* 156: 2553–2557
- Harada H, Willison K, Sakakibara J, Miyamoto M, Fujita T, Taniguchi T (1990) Absence of the type I IFN system in EC cells: transcriptional activator (IRF-1) and repressor (IRF-2) genes are developmentally regulated. *Cell* 63: 303–312

- Harms MJ, Ishibashi J, Wang W, Lim HW, Goyama S, Sato T, Kurokawa M, Won KJ, Seale P (2014) Prdm16 is required for the maintenance of brown adipocyte identity and function in adult mice. *Cell Metab* 19: 593–604
- Harms MJ, Lim HW, Ho Y, Shapira SN, Ishibashi J, Rajakumari S, Steger DJ, Lazar MA, Won KJ, Seale P (2015) PRDM16 binds MED1 and controls chromatin architecture to determine a brown fat transcriptional program. *Genes Dev* 29: 298–307
- Hata N, Sato M, Takaoka A, Asagiri M, Tanaka N, Taniguchi T (2001) Constitutive IFN- α / β signal for efficient IFN- α / β gene induction by virus. *Biochem Biophys Res Commun* 285: 518–525
- Hida S, Ogasawara K, Sato K, Abe M, Takayanagi H, Yokochi T, Sato T, Hirose S, Shirai T, Taki S, Taniguchi T (2000) CD8(+) T cell-mediated skin disease in mice lacking IRF-2, the transcriptional attenuator of interferon- α / β signaling. *Immunity* 13: 643–655
- Honda K, Yanai H, Takaoka A, Taniguchi T (2005) Regulation of the type I IFN induction: a current view. *Int Immunol* 17: 1367–1378
- Horvath CM, Stark GR, Kerr IM, Darnell JE Jr (1996) Interactions between STAT and non-STAT proteins in the interferon-stimulated gene factor 3 transcription complex. *Mol Cell Biol* 16: 6957–6964
- Hwang SY, Hertzog PJ, Holland KA, Sumarsono SH, Tymms MJ, Hamilton JA, Whitty G, Bertoncillo I, Kola I (1995) A null mutation in the gene encoding a type I interferon receptor component eliminates antiproliferative and antiviral responses to interferons α and β and alters macrophage responses. *Proc Natl Acad Sci USA* 92: 11284–11288
- Iida S, Chen W, Nakadai T, Ohkuma Y, Roeder RG (2015) PRDM16 enhances nuclear receptor-dependent transcription of the brown fat-specific Ucp1 gene through interactions with Mediator subunit MED1. *Genes Dev* 29: 308–321
- Ishibashi J, Seale P (2015) Functions of Prdm16 in thermogenic fat cells. *Temperature* 2: 65–72
- Kajimura S, Seale P, Tomaru T, Erdjument-Bromage H, Cooper MP, Ruas JL, Chin S, Tempst P, Lazar MA, Spiegelman BM (2008) Regulation of the brown and white fat gene programs through a PRDM16/CtBP transcriptional complex. *Genes Dev* 22: 1397–1409
- Kajimura S, Seale P, Kubota K, Lunsford E, Frangioni JV, Gygi SP, Spiegelman BM (2009) Initiation of myoblast to brown fat switch by a PRDM16-C/EBP- β transcriptional complex. *Nature* 460: 1154–1158
- Kawashima T, Kosaka A, Yan H, Guo Z, Uchiyama R, Fukui R, Kaneko D, Kumagai Y, You DJ, Carreras J, Uematsu S, Jang MH, Takeuchi O, Kaisho T, Akira S, Miyake K, Tsutsui H, Saito T, Nishimura I, Tsuji NM (2013) Double-stranded RNA of intestinal commensal but not pathogenic bacteria triggers production of protective interferon- β . *Immunity* 38: 1187–1197
- Kim PG, Canver MC, Rhee C, Ross SJ, Harriss JV, Tu HC, Orkin SH, Tucker HO, Daley GQ (2016) Interferon- α signaling promotes embryonic HSC maturation. *Blood* 128: 204–216
- Kimura T, Nakayama K, Penninger J, Kitagawa M, Harada H, Matsuyama T, Tanaka N, Kamijo R, Vilcek J, Mak TW, Taniguchi T (1994) Involvement of the IRF-1 transcription factor in antiviral responses to interferons. *Science* 264: 1921–1924
- Klingenberg M, Echtay KS, Bienengraeber M, Winkler E, Huang SG (1999) Structure-function relationship in UCP1. *Int J Obes Relat Metab Disord* 23 (Suppl. 6): S24–S29
- Kong X, Banks A, Liu T, Kazak L, Rao RR, Cohen P, Wang X, Yu S, Lo JC, Tseng YH, Cypess AM, Xue R, Kleiner S, Kang S, Spiegelman BM, Rosen ED (2014) IRF4 is a key thermogenic transcriptional partner of PGC-1 α . *Cell* 158: 69–83
- Kuleshov MV, Jones MR, Rouillard AD, Fernandez NF, Duan Q, Wang Z, Koplev S, Jenkins SL, Jagodnik KM, Lachmann A, McDermott MG, Monteiro CD, Gunderson GW, Ma'ayan A (2016) Enrichr: a comprehensive gene set enrichment analysis web server 2016 update. *Nucleic Acids Res* 44: W90–W97
- Kumari M, Wang X, Lantier L, Lyubetskaya A, Eguchi J, Kang S, Tenen D, Roh HC, Kong X, Kazak L, Ahmad R, Rosen ED (2016) IRF3 promotes adipose inflammation and insulin resistance and represses browning. *J Clin Invest* 126: 2839–2854
- Kuo TC, Calame KL (2004) B lymphocyte-induced maturation protein (Blimp)-1, IFN regulatory factor (IRF)-1, and IRF-2 can bind to the same regulatory sites. *J Immunol* 173: 5556–5563
- Lee K, Um SH, Rhee DK, Pyo S (2016) Interferon- α inhibits adipogenesis via regulation of JAK/STAT1 signaling. *Biochim Biophys Acta* 1860: 2416–2427
- Lei Q, Liu X, Fu H, Sun Y, Wang L, Xu G, Wang W, Yu Z, Liu C, Li P, Feng J, Li G, Wu M (2016) miR-101 reverses hypomethylation of the PRDM16 promoter to disrupt mitochondrial function in astrocytoma cells. *Oncotarget* 7: 5007–5022
- Leung S, Qureshi SA, Kerr IM, Darnell JE Jr, Stark GR (1995) Role of STAT2 in the alpha interferon signaling pathway. *Mol Cell Biol* 15: 1312–1317
- Lewis JA, Huq A, Najjarro P (1996) Inhibition of mitochondrial function by interferon. *J Biol Chem* 271: 13184–13190
- Li X, Wang J, Jiang Z, Guo F, Soloway PD, Zhao R (2015) Role of PRDM16 and its PR domain in the epigenetic regulation of myogenic and adipogenic genes during transdifferentiation of C2C12 cells. *Gene* 570: 191–198
- Luchsinger LL, de Almeida MJ, Corrigan DJ, Mumau M, Snoeck HW (2016) Mitofusin 2 maintains haematopoietic stem cells with extensive lymphoid potential. *Nature* 529: 528–531
- van Marken Lichtenbelt WD, Vanhomerig JW, Smulders NM, Drossaerts JM, Kemerink GJ, Bouvy ND, Schrauwen P, Teule GJ (2009) Cold-activated brown adipose tissue in healthy men. *N Engl J Med* 360: 1500–1508
- Meraz MA, White JM, Sheehan KC, Bach EA, Rodig SJ, Dighe AS, Kaplan DH, Riley JK, Greenlund AC, Campbell D, Carver-Moore K, DuBois RN, Clark R, Aguet M, Schreiber RD (1996) Targeted disruption of the Stat1 gene in mice reveals unexpected physiologic specificity in the JAK-STAT signaling pathway. *Cell* 84: 431–442
- Moisan A, Lee YK, Zhang JD, Hudak CS, Meyer CA, Prummer M, Zoffmann S, Truong HH, Ebeling M, Kiialainen A, Gerard R, Xia F, Schinzel RT, Amrein KE, Cowan CA (2015) White-to-brown metabolic conversion of human adipocytes by JAK inhibition. *Nat Cell Biol* 17: 57–67
- Mould AW, Morgan MA, Nelson AC, Bikoff EK, Robertson EJ (2015) Blimp1/Prdm1 functions in opposition to Irf1 to maintain neonatal tolerance during postnatal intestinal maturation. *PLoS Genet* 11: e1005375
- Nishikata I, Sasaki H, Iga M, Tateno Y, Imayoshi S, Asou N, Nakamura T, Morishita K (2003) A novel EVI1 gene family, MEL1, lacking a PR domain (MEL1S) is expressed mainly in t(1;3)(p36;q21)-positive AML and blocks G-CSF-induced myeloid differentiation. *Blood* 102: 3323–3332
- Ohno H, Shinoda K, Spiegelman BM, Kajimura S (2012) PPAR γ agonists induce a white-to-brown fat conversion through stabilization of PRDM16 protein. *Cell Metab* 15: 395–404
- Ohno H, Shinoda K, Ohyama K, Sharp LZ, Kajimura S (2013) EHMT1 controls brown adipose cell fate and thermogenesis through the PRDM16 complex. *Nature* 504: 163–167
- Park C, Li S, Cha E, Schindler C (2000) Immune response in Stat2 knockout mice. *Immunity* 13: 795–804
- Petrovic N, Shabalina IG, Timmons JA, Cannon B, Nedergaard J (2008) Thermogenically competent nonadrenergic recruitment in brown preadipocytes by a PPAR γ agonist. *Am J Physiol Endocrinol Metab* 295: E287–E296

- Pinheiro I, Margueron R, Shukeir N, Eisold M, Fritzsche C, Richter FM, Mittler G, Genoud C, Goyama S, Kurokawa M, Son J, Reinberg D, Lachner M, Jenwein T (2012) Prdm3 and Prdm16 are H3K9me1 methyltransferases required for mammalian heterochromatin integrity. *Cell* 150: 948–960
- Rajakumari S, Wu J, Ishibashi J, Lim HW, Giang AH, Won KJ, Reed RR, Seale P (2013) EBF2 determines and maintains brown adipocyte identity. *Cell Metab* 17: 562–574
- Saito M, Okamatsu-Ogura Y, Matsushita M, Watanabe K, Yoneshiro T, Nio-Kobayashi J, Iwanaga T, Miyagawa M, Kameya T, Nakada K, Kawai Y, Tsujisaki M (2009) High incidence of metabolically active brown adipose tissue in healthy adult humans: effects of cold exposure and adiposity. *Diabetes* 58: 1526–1531
- Sato M, Suemori H, Hata N, Asagiri M, Ogasawara K, Nakao K, Nakaya T, Katsuki M, Noguchi S, Tanaka N, Taniguchi T (2000) Distinct and essential roles of transcription factors IRF-3 and IRF-7 in response to viruses for IFN- α / β gene induction. *Immunity* 13: 539–548
- Sato T, Onai N, Yoshihara H, Arai F, Suda T, Ohteki T (2009) Interferon regulatory factor-2 protects quiescent hematopoietic stem cells from type I interferon-dependent exhaustion. *Nat Med* 15: 696–700
- Schafer SL, Lin R, Moore PA, Hiscott J, Pitha PM (1998) Regulation of type I interferon gene expression by interferon regulatory factor-3. *J Biol Chem* 273: 2714–2720
- Seale P, Kajimura S, Yang W, Chin S, Rohas LM, Uldry M, Tavernier G, Langin D, Spiegelman BM (2007) Transcriptional control of brown fat determination by PRDM16. *Cell Metab* 6: 38–54
- Seale P, Bjork B, Yang W, Kajimura S, Chin S, Kuang S, Scime A, Devarakonda S, Conroe HM, Erdjument-Bromage H, Tempst P, Rudnicki MA, Beier DR, Spiegelman BM (2008) PRDM16 controls a brown fat/skeletal muscle switch. *Nature* 454: 961–967
- Seale P, Conroe HM, Estall J, Kajimura S, Frontini A, Ishibashi J, Cohen P, Cinti S, Spiegelman BM (2011) Prdm16 determines the thermogenic program of subcutaneous white adipose tissue in mice. *J Clin Invest* 121: 96–105
- Shalem O, Sanjana NE, Hartenian E, Shi X, Scott DA, Mikkelsen TS, Heckl D, Ebert BL, Root DE, Doench JG, Zhang F (2014) Genome-scale CRISPR-Cas9 knockout screening in human cells. *Science* 343: 84–87
- Shan B, Vazquez E, Lewis JA (1990) Interferon selectively inhibits the expression of mitochondrial genes: a novel pathway for interferon-mediated responses. *EMBO J* 9: 4307–4314
- Tai TA, Jennermann C, Brown KK, Oliver BB, MacGinnitie MA, Wilkison WO, Brown HR, Lehmann JM, Kliewer SA, Morris DC, Graves RA (1996) Activation of the nuclear receptor peroxisome proliferator-activated receptor gamma promotes brown adipocyte differentiation. *J Biol Chem* 271: 29909–29914
- Tovey MG, Streuli M, Gresser I, Gugenheim J, Blanchard B, Guymarho J, Vignaux F, Gigou M (1987) Interferon messenger RNA is produced constitutively in the organs of normal individuals. *Proc Natl Acad Sci USA* 84: 5038–5042
- Vogel SN, Fertsch D (1984) Endogenous interferon production by endotoxin-responsive macrophages provides an autostimulatory differentiation signal. *Infect Immun* 45: 417–423
- Wang XA, Zhang R, Zhang S, Deng S, Jiang D, Zhong J, Yang L, Wang T, Hong S, Guo S, She ZG, Zhang XD, Li H (2013) Interferon regulatory factor 7 deficiency prevents diet-induced obesity and insulin resistance. *Am J Physiol Endocrinol Metab* 305: E485–E495
- Xu L, Zhou X, Wang W, Wang Y, Yin Y, van der Laan LJ, Sprengers D, Metselaar HJ, Peppelenbosch MP, Pan Q (2016) IFN regulatory factor 1 restricts hepatitis E virus replication by activating STAT1 to induce antiviral IFN-stimulated genes. *FASEB J* 30: 3352–3367
- Yu Q, Katlinskaya YV, Carbone CJ, Zhao B, Katlinski KV, Zheng H, Guha M, Li N, Chen Q, Yang T, Lengner CJ, Greenberg RA, Johnson FB, Fuchs SY (2015) DNA-damage-induced type I interferon promotes senescence and inhibits stem cell function. *Cell Rep* 11: 785–797
- Zhou B, Wang J, Lee SY, Xiong J, Bhanu N, Guo Q, Ma P, Sun Y, Rao RC, Garcia BA, Hess JL, Dou Y (2016) PRDM16 suppresses MLL1r leukemia via intrinsic histone methyltransferase activity. *Mol Cell* 62: 222–236